Immunology
The Journal of cells, molecules, systems and technologies

British Society for immunology

IMMUNOLOGY ORIGINAL ARTICLE

Inhibition of the Fibrinogen-Like Protein 2:FcγRIIB/RIII immunosuppressive pathway enhances antiviral T-cell and B-cell responses leading to clearance of lymphocytic choriomeningitis virus clone 13

Olga Luft,[1] Ramzi Khattar,[1] Kaveh Farrokhi,[2] Dario Ferri,[2] Nataliya Yavorska,[1] Jianhua Zhang,[1] Hassan Sadozai,[1] Oyedele Adeyi,[1] Andrzej Chruscinski,[1] Gary A. Levy[1,2] and Nazia Selzner[1]

[1]*Toronto General Hospital, Multi Organ Transplant Programme, Toronto, ON, Canada and* [2]*Department of Immunology, University of Toronto, Toronto, ON, Canada*

doi:10.1111/imm.12897
Received 19 June 2017; revised 31 October 2017; accepted 10 January 2018.
O.K. and R.K. contributed equally to this work.
Correspondence: Dr Nazia Selzner, Toronto General Hospital, NCSB 11C-1244, 585 University Avenue, Toronto ON M5G 2N2, Canada. Email: Nazia.Selzner@uhn.ca
Senior author: Dr. Nazia Selzner

Summary

Persistent viruses evade immune detection by interfering with virus-specific innate and adaptive antiviral immune responses. Fibrinogen-like protein-2 (FGL2) is a potent effector molecule of $CD4^+$ $CD25^+$ $FoxP3^+$ regulatory T cells and exerts its immunosuppressive activity following ligation to its cognate receptor, FcγRIIB/RIII. The role of FGL2 in the pathogenesis of chronic viral infection caused by lymphocytic choriomeningitis virus clone-13 (LCMV cl-13) was assessed in this study. Chronically infected $fgl2^{+/+}$ mice had increased plasma levels of FGL2, with reduced expression of the maturation markers, CD80, CD86 and MHC-II on macrophages and dendritic cells and impaired production of neutralizing antibody. In contrast, $fgl2^{-/-}$ mice or $fgl2^{+/+}$ mice that had been pre-treated with antibodies to FGL2 and FcγRIIB/RIII and then infected with LCMV cl-13 developed a robust $CD4^+$ and $CD8^+$ antiviral T-cell response, produced high titred neutralizing antibody to LCMV and cleared LCMV. Treatment of mice with established chronic infection with antibodies to FGL2 and FcγRIIB/RIII was shown to rescue the number and functionality of virus-specific $CD4^+$ and $CD8^+$ T cells with reduced total and virus-specific T-cell expression of programmed cell death protein 1 leading to viral clearance. These results demonstrate an important role for FGL2 in viral immune evasion and provide a rationale to target FGL2 to treat patients with chronic viral infection.

Keywords: chronic infection; fibrinogen-like protein 2; T-cell exhaustion.

Introduction

Human chronic viral infections including, hepatitis B virus (HBV), hepatitis C virus (HCV) and human immunodeficiency virus (HIV) represent serious global health problems.[1,2] Lymphocytic choriomeningitis virus clone-13 (LCMV cl-13) has been used as a model to gain insight into the mechanisms that contribute to viral persistence. In LCMV cl-13 infection, early exposure to high viral loads leads to increased expression of inhibitory receptors, including programmed cell death protein-1 (PD-1),[3] prostaglandin E_2 receptors,[4] cytotoxic T-lymphocyte-associated protein-4[5] and T-cell immunoglobulin mucin-3[6] on activated T cells, and expression of immunosuppressive cytokines including interleukin-10 and transforming growth factor-β, leading to T-cell and B-cell dysfunction.[7,8] It is known that virus-specific T cells are present in patients with chronic infections;

Abbreviations: APC, antigen-presenting cells; DC, dendritic cells; FGL2, fibrinogen-like protein 2; FITC, fluorescein isothiocyanate; HBV, hepatitis B virus; HCV, hepatitis C virus; IFN-γ, interferon-γ; LCMV cl-13, lymphocytic choriomeningitis virus clone-13; PD-1, programmed cell death protein-1; PE, phycoerythrin; PerCP, peridinin chlorophyll protein; PFU, plaque-forming units; p.i., post infection; Th1, T helper type 1; TIGIT, T-cell immunoreceptor with immunoglobulin and immunoreceptor tyrosine-based inhibition motif domains; TNF-α, tumour necrosis factor-α; Treg cell, $CD4^+$ $CD25^+$ $FoxP3^+$ regulatory T cell

however, they are functionally exhausted (T-cell exhaustion). In T-cell exhaustion,[9] virus-specific cytotoxic T lymphocytes have diminished cytotoxic effector activity, progressively lose effector cytokine secretion of interleukin-2, tumour necrosis factor-α (TNF-α) and interferon-γ (IFN-γ),[10] have decreased proliferative capacity[11] and can be physically deleted from the immune repertoire.[12] Treatment with antibodies to PD-1 : programmed death ligand 1 or the receptor to interleukin-10 has been reported to prevent T-cell exhaustion and lead to clearance of LCMV cl-13.[3,13–15] The effects of T-cell exhaustion have been shown to be reversible and more importantly responsive to treatment, making T-cell exhaustion a prime target for therapeutic intervention to improve treatment of patients with chronic viral infection.[13,14,16]

$CD4^+$ $CD25^+$ $FoxP3^+$ regulatory T (Treg) cells are known to contribute to viral persistence through inhibition of both innate and adaptive immunity.[17–19] Previous studies have shown that depletion of Treg cells enhances immunity against HBV[20] and HCV.[21] Recently, a subset of inducible and natural Treg cells expressing the T-cell immunoreceptor with immunoglobulin and immunoreceptor tyrosine-based inhibition motif domains (TIGIT) have been identified.[22] Ligation of TIGIT to CD155 on antigen-presenting cells (APC) leads to increased expression of FGL2, resulting in suppression of both T helper type 1 (Th1) and Th17 responses *in vivo*.[22] We and others have shown that FGL2 exerts its immunosuppressive activity following binding to its cognate receptor FcγRIIB/RIII, which is expressed on APC, natural killer cells and B cells. Although it has been shown that naive T cells do not express FcγRIIB/RIII, in the setting of viral infection, activated T cells may express FcγRIIB/RIII. Hence, in chronic viral disease, the T-cell inhibitory effects may be both direct and indirect.[23–25]

Engagement of Fcγ receptors have been implicated in the pathogenesis of a number of immunologically mediated diseases[26–28] and regulates the response to parasitic[29] and bacterial[30,31] infections. We and others have reported that FGL2 contributes to the pathogenesis of fulminant viral hepatitis induced by mouse hepatitis virus-3 and an acute self-limiting viral hepatitis caused by LCMV WE.[22,32,33]

In the current study, we used two complementary but independent approaches to evaluate whether inhibition of FGL2 would restore innate and adaptive immunity leading to clearance of chronic LCMV cl-13 infection. We first showed that targeted deletion of *fgl2* ($fgl2^{-/-}$) enhanced maturation of macrophage and dendritic cells (DC), antiviral T-cell and B-cell immunity, resulting in clearance of chronic LCMV cl-13 infection. Second, the use of neutralizing antibodies to FGL2 and the receptor for FGL2, FcγRIIB/RIII, both before infection and during established chronic infection restored $CD4^+$ and $CD8^+$ T-cell responses, resulting in clearance of LCMV cl-13. These studies confirm the role of FGL2 in chronic viral persistence and the potential to disrupt the FGL2-FcγRIIB/RIII pathway as a novel therapeutic strategy to treat humans with chronic infections.

Materials and methods

Mice

The $fgl2^{-/-}$ mice were generated as described previously.[34] Eight- to ten-week-old weight-matched C57BL/6 littermate $fgl2^{+/+}$ and $fgl2^{-/-}$ female mice received 2×10^6 plaque-forming units (PFU) of LCMV cl-13. Animal protocols were approved by the University Health Network in accordance with guidelines set by the Canadian Council on Animal Care.

LCMV virus and viral titres

LCMV cl-13 was obtained as a gift from the laboratory of Dr M. Oldstone (The Scripps Research Institute, La Jolla, CA) and was propagated in BHK-21 cells (ATCC # CCL-10).[15] Mice were infected intravenously with LCMV and at defined time-points blood samples were collected into heparinized microvettes (Sarstedt, Nümbrecht, Germany) as previously described.[33] Blood was centrifuged and plasma was collected. Tissues were harvested and snap-frozen in liquid nitrogen. Viral titres were determined on MC57 cells (ATCC # CRL-2295) using focus-forming assay.[35]

Total LCMV-specific IgG detection

An LCMV antibody ELISA was used for the detection of total LCMV-specific antibodies.[36] The absorbance value measured at 450 nm correlated with the captured total LCMV-specific antibody within plasma samples. The dilution series for each plasma sample was plotted and read where the dilution and observed absorbance values had a linear relationship with one another. Samples were expressed as a fold increase from naive absorbance.

Neutralizing antibody detection

LCMV neutralizing antibody titres were quantified in plasma from LCMV cl-13 infected mice using a plaque reduction assay.[37] Plasma was diluted 1 : 10 in complete α-modified Eagle's minimum essential medium supplemented with 2% fetal bovine serum and was serially diluted and mixed with 100 PFU of LCMV cl-13 for 1 hr at 37°. Following incubation, samples were added to MC57 cells and plaques were visualized using a standard focus-forming assay.[35]

LCMV ex vivo peptide re-stimulation

Splenic mononuclear cells were isolated as previously described[38] and stimulated with 10 μg/ml of the MHC

class I peptide glycoprotein GP_{33-41} or nucleoprotein $NP_{396-404}$ for 6 hr as previously described.[39–41] The LCMV peptide GP_{33-41} H-2Db (KAVYNFATC) and $NP_{396-404}$ H-2Db (FQPQNGQFI) was synthesized by Anaspec Inc. (Fremont, CA). Brefeldin A (Sigma-Aldrich, St Louis, MO) was added to cultures after 1 hr of peptide re-stimulation for 5 hr at a final concentration of 10 μg/ml. Flow cytometry was used to assess the frequency of splenic mononuclear cells producing IFN-γ following *ex vivo* peptide re-stimulation.

Macrophage and DC isolation

Macrophages ($CD11b^+$ $NK1.1^-$) and DC ($CD11c^+$) were isolated as previously described.[33,42] Following incubation for 20 min with 5% mouse serum (Cedarlane Laboratories, Burlington, ON, Canada) in PBS at 4°, splenic mononuclear cells were fixed with 2% paraformaldehyde in PBS solution (Santa Cruz Biotechnology, Dallas, TX) for 20 min and stained with antibodies and gated as shown in the Supplementary material (Fig. S1).

Flow cytometry

Antibodies. Antibodies used for flow cytometry: The following antibodies were purchased from eBioscience (San Diego, CA) and were used to stain cells for FACS analysis as described below: Peridinin chlorophyll protein (PerCP) -Cy5.5-CD3ε (Clone 17A2), fluorescein isothiocyanate (FITC) -CD4 (Clone GK1.5), phycoerythrin (PE) -CD8α (Clone 53-6.7), PerCP-Cy5.5-CD11b (Clone M1/70), allophycocyanin-CD80 (Clone 16-10A1), PE-MHC-II (I-A) (Clone NIMR-4), FITC-CD86 (Clone GL-1), FITC-IFN-γ (Clone XMG1.2), PerCP-Cy5.5-TNF-α (Clone MP6-XT22), CD16/CD32 (Clone 93), PE-CD11c (Clone N418), FITC-CD45R (Clone RA3-6B2), PE-CD19 [eBio1D3(1D3)] and PE-NK1.1 (Clone PK136). Fixable viability dye eFluor 450 (eBioscience) was used, diluted 1 : 1000, as the viability dye.

Tetramers. Biotinylated MHC-I monomers ($GP_{33–41}$) were provided by the NIH Tetramer Core Facility, Emory University (Atlanta, GA). MHC-I monomers were tetramerized with streptavidin-PE according to NIH Tetramer Core Facility instructions. Fixable viability dye eFluor 450 (eBioscience) was used to confirm cell viability. Tetramer staining was performed on freshly isolated and unstimulated cells.

Cell staining. Mononuclear cells were isolated from the spleen, washed and resuspended in FACS buffer (PBS containing 1% fetal calf serum and 1 mM EDTA) at a final concentration of 1×10^7 cells/ml. Cells were treated with CD16/CD32 to block non-specific binding to Fc-receptors. Cells were surface stained with antibodies and LCMV-specific tetramers. Cells were then fixed with 2% paraformaldehyde. FACS analysis was performed using a BD LSRII Flow Cytometer and data were analysed using FlowJo software (Tree Star Inc., Ashland, OR). Live cells were discriminated according to forward-scatter and side-scatter parameters and a fixable viability dye (eBioscience).

In vivo antibody treatment

The monoclonal antibody 9D8 was generated as previously described.[43] The effects of 9D8 on both the innate and adaptive immune systems are shown in the Supplementary material (Fig. S2). Anti-mouse FcγRIIB/RIII (clone 2.4G2 ATCC HB-197) was purchased from the American Tissue Culture Centre (Manassas, VA). Studies were undertaken to determine if antibody to FGL2, FcγRIIB/RIII alone or in combination could prevent the development of chronic infection or treat established chronic infection. The $fgl2^{+/+}$ mice were divided into five groups ($n > 5$/group) and treated with 150 μg of anti-FGL2 monoclonal antibody (9D8) (Group 1); 150 μg of anti-FcγRIIB/RIII monoclonal antibody (2.4G2) (Group 2); 150 μg of 9D8 and 150 μg 2.4G2 (Group 3) or with 150 μg mouse IgG1 isotype control antibody (clone MOPC-21) and 150 μg of rat IgG2A isotype control antibody (clone 2A3) (Group 4) or PBS alone (Group 5). For studies to determine if antibody to FGL2 could prevent progression to chronic disease, antibody was initiated 2 days before infection and continued every 2 days until day 20 post infection (p.i.) and then given at days 23, 26, 32 and 45 p.i. until the mice were killed on day 56 p.i. To determine if antibody treatment was effective in established chronic infection, treatment with antibody was initiated at day 25 p.i. and continued every second day until death on day 56 p.i.

FGL2 ELISA

Plasma levels of FGL2 were quantified as previously described.[33] Briefly, plates were coated and incubated overnight with 1 ng/ml monoclonal anti-FGL2 (6H12) (IgG1) as a capture antibody. Plasma samples (50 μl) were added to each well, and following 1 hr incubation at 37° and three washes with Tris-buffered saline, the wells were incubated with 2 μg/ml polyclonal rabbit anti-FGL2 antibody for 2 hr at 37°. The plate was washed again and polyclonal anti-FGL2 binding was detected with secondary horseradish peroxidase-conjugated anti-rabbit antibody. Tetrametylbenzidine was then added and absorbance was measured at 450 nm using an ELISA plate reader. Levels of FGL2 were undetectable in the plasma of $fgl2^{-/-}$ mice both before and after LCMV infection.

Immunohistochemistry and morphometric analysis

The $fgl2^{+/+}$ mice and $fgl2^{-/-}$ mice were infected intravenously with 2×10^6 PFU of LCMV cl-13. Tissues were frozen in Optimal Cutting Temperature compound (Sakura Finetek, Alphen aan den Rijn, the Netherlands) and 5-μm thick tissue sections were stained with a rat antibody to the nucleoprotein of LCMV (VL4) provided as a gift from Dr P. Ohashi (Princess Margaret Hospital, Toronto, ON, Canada). The tissues were then incubated with a horseradish peroxidase-conjugated secondary anti-rat IgG antibody that allowed for colour development after addition of substrate 3,3′-diaminobenzidine (Zymed, San Francisco, CA). Morphometric analysis for LCMV nucleoprotein (NP) was performed in liver at days 28 and 56 p.i. as previously described.[33] Slides were digitally scanned and the number of LCMV NP^+ cells was quantified by morphometric analysis using Spectrum V.10.2.2.2317 (Aperio Technologies Inc., Vista, CA). The number of LCMV NP^+ cells was expressed as a percentage of total cells. Control uninfected $fgl2^{+/+}$ and $fgl2^{-/-}$ livers were used as a control and did not stain positive for LCMV NP.

Statistics

Statistical significance was assessed using the analysis of variance or a Student's *t*-test. Statistical analysis was performed using Prism 5 software (Graphpad Software Inc., San Diego, CA). Differences with $P \leq 0{\cdot}05$ were considered statistically significant.

Results

LCMV cl-13 infection leads to increased expression of FGL2

Following infection with 2×10^6 PFU of LCMV cl-13 intravenously, increased plasma levels of FGL2 were detected in $fgl2^{+/+}$ mice by day 7 p.i., reaching maximum levels on day 10 p.i. (52-fold) and remained persistently elevated until day 56 p.i., although differences were only statistically significant until day 42 p.i. (Fig. 1).

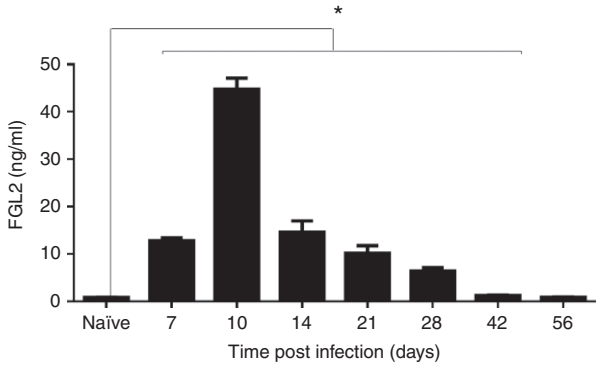

Figure 1. Chronic infection by lymphocytic choriomeningitis virus clone 13 (LCMV cl-13) induces the expression of fibrinogen-like protein 2 (FGL2). $Fgl2^{+/+}$ mice were infected with 2×10^6 PFU of LCMV cl-13 intravenously and levels of FGL2 were measured in the plasma by ELISA. Graphs represent the mean ± SEM of five mice per time-point from two independent experiments $*P < 0{\cdot}05$.

Targeted deletion of *fgl2* leads to clearance of LCMV cl-13

To examine the effect of deletion of *fgl2* on viral clearance, both $fgl2^{+/+}$ and $fgl2^{-/-}$ mice were infected intravenously with LCMV cl-13 and viral titres were measured in plasma (Fig. 2a), lung (Fig. 2b) and liver (Fig. 2c) using a focus-forming assay. On day 28 p.i., the titres of LCMV cl-13 were significantly lower in the plasma ($P < 0{\cdot}005$), lung ($P < 0{\cdot}05$) and liver ($P < 0{\cdot}005$) of $fgl2^{-/-}$ mice compared with $fgl2^{+/+}$ mice. Furthermore, by day 56 p.i., all $fgl2^{-/-}$ mice had undetectable virus from the lung, liver and plasma whereas $fgl2^{+/+}$ mice remained persistently infected. To confirm that $fgl2^{-/-}$ mice had cleared LCMV cl-13, liver tissues were stained for LCMV nucleoprotein and the percentage of $LCMV^+$ cells was analysed by morphometric analysis at days 28 and 56 p.i. Consistent with the focus-forming assay, morphometric analysis revealed that LCMV antigen was undetectable in the livers of $fgl2^{-/-}$ mice at day 56 p.i., whereas LCMV NP antigen was detected in $fgl2^{+/+}$ mice indicating LCMV cl-13 viral clearance in $fgl2^{-/-}$ mice (Fig. 2d,e).

Targeted deletion of *fgl2* leads to increased numbers of macrophages and DC expressing CD80, CD86 and MHC-II

To study the effects of FGL2 on APC maturation after LCMV cl-13 infection, DC ($CD11c^+$) and macrophages ($CD11b^+$, $NK1.1^-$) were isolated from the spleen of $fgl2^{+/+}$ and $fgl2^{-/-}$ mice both before infection and at day 2 p.i. Before infection, macrophage (Fig. 3a) and DC (Fig. 3c) expression of CD80, CD86 and MHC-II were equivalent in DCs and macrophages isolated from both $fgl2^{+/+}$ and $fgl2^{-/-}$ mice. However, on day 2 p.i., the total number of macrophages and DC expressing CD80, CD86 and MHC-II were significantly increased in $fgl2^{-/-}$ mice compared with $fgl2^{+/+}$ mice (Fig. 3b,d) indicating enhanced maturation of APC isolated from $fgl2^{-/-}$ mice p.i.

Targeted deletion of *fgl2* leads to increased numbers of virus-specific $CD8^+$ T cells following infection with LCMV cl-13

To determine whether FGL2 affected the number of LCMV-specific $CD8^+$ T cells, $fgl2^{-/-}$ mice and $fgl2^{+/+}$ mice were infected with 2×10^6 PFU of LCMV cl-13

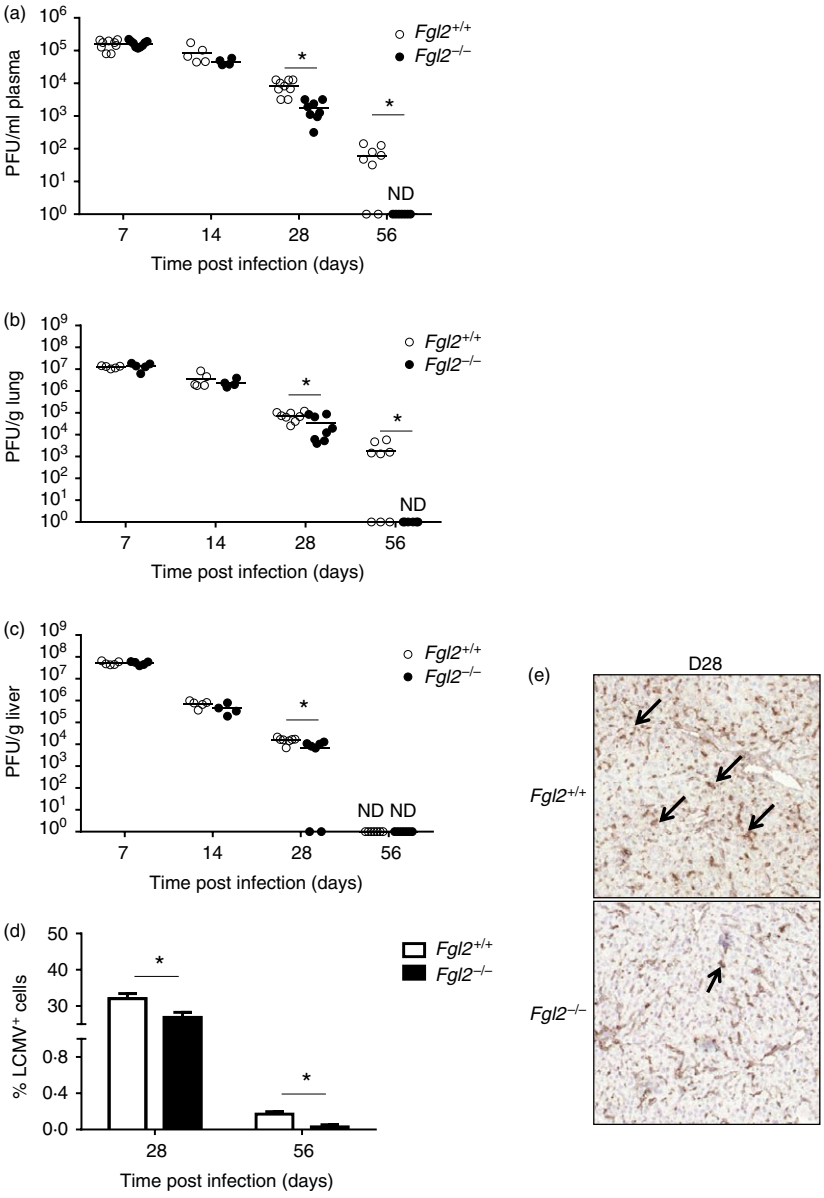

Figure 2. *Fgl2*$^{-/-}$ mice clear lymphocytic choriomeningitis virus clone 13 (LCMV cl-13) in contrast to *fgl2*$^{+/+}$ mice. The *fgl2*$^{+/+}$ and *fgl2*$^{-/-}$ mice were infected with 2×10^6 PFU of LCMV cl-13. Viral titres were measured in plasma (a), lung (b) and liver (c) using an LCMV focus-forming assay. Data are presented as the mean ± SEM of five mice per group and per time-point from two independent experiments $^*P < 0{\cdot}05$. The limit of detection of the LCMV focus-forming assay is denoted by the dashed line. Morphometric analysis for LCMV nucleoprotein in the liver was performed at day 28 and 56 post infection (p.i.) (d). Graph shows the mean ± SEM of four to eight mice per group from one experiment per time-point. $^*P < 0{\cdot}05$. (e) Representative photomicrograph of LCMV-infected liver from *fgl2*$^{+/+}$ and *fgl2*$^{-/-}$ at day 28 p.i. Livers were recovered on day 28 p.i., embedded in OCT and snap frozen. Tissue sections were cut into 5-μm-thick sections and stained with a rat anti-LCMV nucleoprotein (NP) antibody (VL-4). Tissue was incubated with a secondary anti-rat antibody conjugated with horseradish peroxidase that stained positive cells brown after addition of the substrate (3,3′-diaminobenzadine. Marked deposits of LCMV-NP (black arrow) were seen in the hepatocytes and endothelial cells of *fgl2*$^{+/+}$ in comparison with *fgl2*$^{-/-}$ mice (100× magnification). [Colour figure can be viewed at wileyonlinelibrary.com]

intravenously and on days 7, 28 and 56 p.i., splenic mononuclear cells were isolated and stained with the MHC-I tetramer glycoprotein $GP_{33–41}$ to determine the number of LCMV-specific CD8$^+$ T cells. Before infection, CD8$^+$ $Tet_{GP33-41}{}^+$ T cells were undetectable in both *fgl2*$^{+/+}$ mice and *fgl2*$^{-/-}$ mice (data not shown). On day 7 p.i., increased numbers of CD8$^+$ $Tet_{GP33-41}{}^+$ T cells were detected in both *fgl2*$^{+/+}$ and *fgl2*$^{-/-}$ mice. Thereafter, the number of CD8$^+$ $Tet_{GP33-41}{}^+$ T cells from *fgl2*$^{+/+}$ mice contracted both on day 28 and 56 compared with day 7. In contrast, numbers of CD8$^+$ $Tet_{GP33-41}{}^+$ T cells from *fgl2*$^{-/-}$ mice persisted at near equivalent levels at days 7 and 28, and were significantly increased at day 56 compared with *fgl2*$^{+/+}$ mice (Fig. 4a,b).

The effects of targeted deletion of *fgl2* on LCMV-specific CD8$^+$ T-cell effector function was determined by measurement of IFN-γ and TNF-α production in CD8$^+$ T cells following *ex vivo* peptide re-stimulation with the MHC-I-restricted peptide GP_{33-41}. The number of CD8$^+$ T cells producing TNF-α and both TNF-α and IFN-γ in response to *ex vivo* peptide re-stimulation was maximal at day 7 p.i. but was still detectable on day 28 and day 56 p.i. in both *fgl2*$^{+/+}$ mice and *fgl2*$^{-/-}$ mice (data not shown).

Fgl2$^{-/-}$ mice have reduced frequencies of PD-1 expressing CD4$^+$ and CD8$^+$ T cells after LCMV cl-13 infection

We next examined the effect of targeted deletion of *fgl2* on expression of PD-1 after LCMV infection. At baseline, the number of PD-1$^+$ CD4$^+$ and CD8$^+$ T cells was less

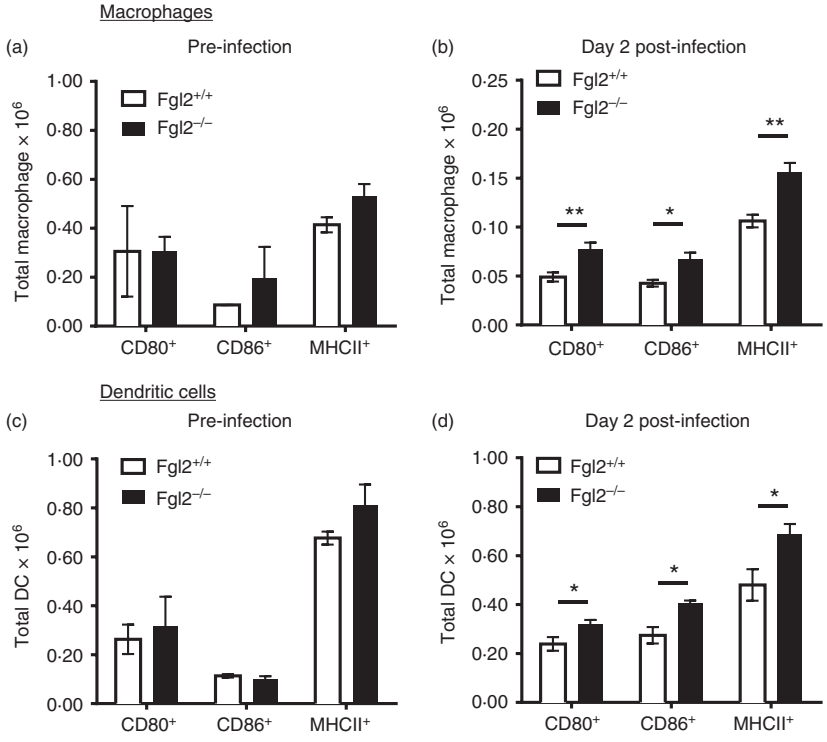

Figure 3. Targeted deletion of *fgl2* leads to increased maturation of macrophages and dendritic cells after lymphocytic choriomeningitis virus clone 13 (LCMV cl-13) infection. Macrophages and dendritic cells were isolated from the spleen of $fgl2^{+/+}$ mice and $fgl2^{-/-}$ before infection and on day 2 p.i. with 2×10^6 PFU of LCMV cl-13. The number of macrophages ($CD11b^+$ $NK1{\cdot}1^-$ cells) (a, b) and number of dendritic cells ($CD11c^+$) (c, d) expressing CD80, CD86 and MHC-II were determined both before and on day 2 post infection by flow cytometry. Data are presented as the mean ± SEM of five mice per group and per time-point from one independent experiment $^*P < 0{\cdot}05$.

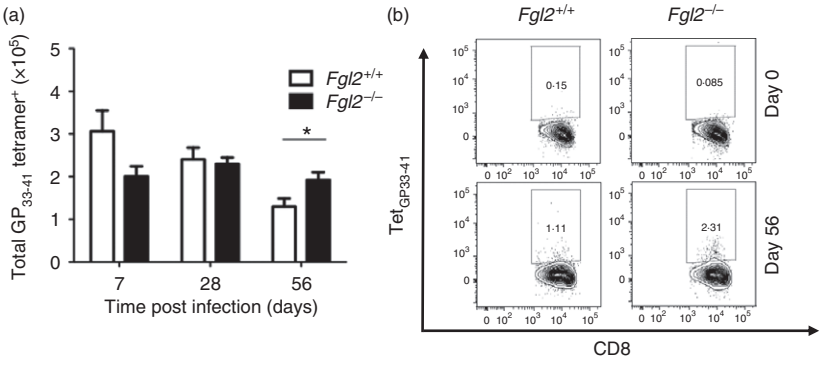

Figure 4. The $fgl2^{-/-}$ mice have increased numbers of virus-specific T cells to lymphocytic choriomeningitis virus (LCMV). Both $fgl2^{+/+}$ and $fgl2^{-/-}$ mice were infected with 2×10^6 PFU of LCMV cl-13 and the number of splenic $CD3^+$ $CD8^+$ $Tet_{GP33\text{-}41}{}^+$ cells were assessed at days 7, 28 and 56 post infection (p.i.) (a). Representative flow plots showing the frequency of $CD8^+$ $Tet_{GP33\text{-}41}{}^+$ gated on $CD3^+$ $CD8^+$ T cells isolated from both $fgl2^{+/+}$ and $fgl2^{-/-}$ mice at days 0 and 56 p.i. are shown (b). Data are presented as the mean ± SEM of five mice per group and per time-point from two independent experiments $^*P < 0{\cdot}05$.

than 10% and near equivalent in $fgl2^{-/-}$ and $fgl2^{+/+}$ mice. However, after LCMV infection, the number of $CD4^+$ PD-1^+ T cells was reduced in $fgl2^{-/-}$ mice compared with $fgl2^{+/+}$ mice (Fig. 5a,b). In contrast to $CD4^+$ cells, the number of PD-1^+ $CD8^+$ T cells was only reduced in $fgl2^{-/-}$ mice compared with $fgl2^{+/+}$ mice at day 56 and day 100 p.i. (Fig. 5c,d). Furthermore, the frequency of $CD8^+$ $Tet_{GP33\text{-}41}{}^+$ T cells expressing PD-1 was reduced in $fgl2^{-/-}$ mice compared with $fgl2^{+/+}$ mice (Fig. 5e,f). Collectively, these data demonstrate that deletion of *fgl2* leads to increased numbers of pro-inflammatory LCMV-specific $CD8^+$ T cells and a reduced percentage of PD-1-expressing $CD4^+$ and $CD8^+$ T cells after LCMV cl-13 infection.

$Fgl2^{-/-}$ mice generate increased numbers of T-cell memory cells and increased neutralizing antibody titres

To assess virus-specific memory, splenic mononuclear cells were isolated from virus-infected mice and assessed by flow cytometry according to the gating strategy in the

Supplementary material (Fig. S3). The total number of $CD8^+$ effector memory (Fig. 6a), $CD4^+$ effector memory (Fig. 6c), $CD8^+$ central memory (Fig. 6e) and $CD4^+$ central memory (Fig. 6f) cells was near equivalent in both *fgl2*$^{-/-}$ and *fgl2*$^{+/+}$ uninfected mice. At day 56 following infection, *fgl2*$^{-/-}$ mice had a 1·8-fold increase in the number of $CD8^+$ effector memory cells (Fig. 6a); a 1·7-fold increase in $CD8^+$ $Tet_{Gp33\text{-}41}{}^+$ effector memory cells (Fig. 6b); a twofold increase in $CD4^+$ effector memory cells (Fig. 6c); a 21-fold increase in $CD4^+$ $Tet_{GP61\text{-}80}{}^+$ effector memory cells (Fig. 6d); a twofold increase in $CD8^+$ central memory cells (Fig. 6e) and a 2·8-fold increase in $CD4^+$ central memory cells (Fig. 6f) compared with *fgl2*$^{+/+}$ mice. There were elevated levels of $CD4^+$ $Tet_{GP61\text{-}80}{}^+$ and $CD8^+$ $Tet_{Gp33\text{-}41}{}^+$ central memory in *fgl2*$^{-/-}$ mice, but these did not reach statistical significance (data not shown).

Total IgG antibody to LCMV was near equivalent in both *fgl2*$^{+/+}$ and *fgl2*$^{-/-}$ mice and was first detected on day 7 p.i. and persisted until day 56 p.i. (Fig. 7a). In contrast, neutralizing antibody to LCMV was detected at day 56 and continued to increase to day 130 p.i. in *fgl2*$^{-/-}$ mice (Fig. 7b). On day 70 p.i., neutralizing antibody was detected in both strains of mice, but the titre was significantly higher in *fgl2*$^{-/-}$ mice. Neutralizing antibody persisted until 130 days p.i. but at significantly higher titres in *fgl2*$^{-/-}$ mice. Hence, while both *fgl2*$^{+/+}$ and *fgl2*$^{-/-}$ mice produced antibodies to LCMV, only *fgl2*$^{-/-}$ generated neutralizing antibodies until day 56.

To determine that antibody treatment could prevent the development of chronic LCMV infection, mice were pre-treated with either PBS, isotype control antibodies, anti-FGL2 (9D8) or anti-FcγRIIB /RIII (2.4G2) antibody alone, which had minimal effect on T-cell antiviral responses and none of these mice cleared LCMV cl-13 (data not shown). In contrast, pre-treatment of *fgl2*$^{+/+}$ mice with combination antibodies to FGL2 (9D8) and to FcγRIIB/RIII (2.4G2) led to viral clearance (Fig. 8a). Treated mice had a 3·4-fold increase in numbers of $CD8^+$ $Tet_{GP33\text{-}41}{}^+$ T cells (Fig. 8b) and a 2·3-fold and twofold increase in numbers of IFN-γ^+ $CD8^+$ T cells to *ex vivo* peptide re-stimulation with the MHC-I-restricted peptides $GP_{33\text{-}41}$ and $NP_{396\text{-}404}$, respectively, in comparison with PBS and isotype control treated mice (Fig. 8c). The number of $CD8^+$ T cells expressing PD-1 in LCMV-infected *fgl2*$^{+/+}$ mice treated with anti-FGL2 and anti-FcγRIIB/RIII was also reduced compared with PBS and isotype control treated mice (Fig. 8d).

To examine whether antibodies to both FGL2 and FcγRIIB/RIII could be an effective treatment for chronic infection, *fgl2*$^{+/+}$ mice, which had been previously infected with 2×10^6 PFU of LCMV cl-13 and had developed chronic disease, were treated on day 25 p.i. with 150 μg of 9D8 and 2.4G2 or PBS. Treatment was continued every 2 days until death on day 56 p.i.[44] At day 56 p.i., the number of $CD3^+$ $CD8^+$ $Tet_{GP33\text{-}41}{}^+$ in antibody- or PBS-treated mice was equivalent (Fig. 9a). Total $CD3^+$ $CD8^+$ $Tet_{NP396\text{-}404}{}^+$ and $CD3^+$ $CD4^+$ $Tet_{GP61\text{-}80}{}^+$ were significantly increased in 2.4G2/9D8 antibody-treated mice compared with control mice (Fig. 9a). $CD4^+$ and $CD8^+$ T cells from 2.4G2/9D8-treated mice produced increased amounts of IFN-γ (Fig. 9b) and TNF-α in response to *ex vivo* peptide re-stimulation with $GP_{33\text{-}41}$, $NP_{396\text{-}404}$ or $GP_{61\text{-}80}$ in contrast to PBS controls (Fig. 9c). The number of $CD3^+$ $CD8^+$ (Fig. 9d) and $CD3^+$ $CD4^+$ T cells (Fig. 9e) expressing PD-1 was also significantly reduced in 2.4G2/9D8-treated mice. The frequency (%) of LCMV-specific ($Tet_{GP33\text{-}41}{}^+$) $CD8^+$ T cells expressing PD-1 was also reduced in antibody-treated mice (Fig. 9f). All mice treated with 2.4G2/9D8 cleared LCMV cl-13 by day 56 whereas PBS-treated control mice remained chronically infected (Fig. 9g).

Discussion

Effective viral clearance requires a robust innate and adaptive antiviral immune response.[15,44] A common feature of chronic infection is the lack of virus-specific T-cell responses, which is characterized by progressive functional T-cell exhaustion and deletion of virus-specific $CD4^+$ and $CD8^+$ T cells. Accounting at least in part for T-cell exhaustion is the overproduction of Treg cells[45] with a shift in the ratio of T-cell sustaining pro-inflammatory cytokines including interleukin-2,[46,47] IFN-γ and TNF-α[48] and increased production of anti-inflammatory cytokines including interleukin-10.[15] FGL2 has been identified as an important immunosuppressive effector of Treg cells and central to the suppressive function of a major subset of $CD4^+$ $CD25^+$ $FoxP3^+$ Treg cells expressing TIGIT.[32,34,49,50] Ligation of TIGIT to CD155 on APC leads to increased expression of FGL2, resulting in suppression of both Th1 and Th17 responses *in vivo*.[22] We and others have shown that FGL2 exerts its immunosuppressive activity following binding to FcγRIIB/RIII, which is expressed primarily on APC.[49] The data generated in Fig. 4 show that the differences between *fgl2*$^{+/+}$ mice and *fgl2*$^{-/-}$ mice emerge late in LCMV infection, which supports the contention that enhanced maturation of APC early in infection does not result in early priming of T cells, but rather is involved in the maintenance of virus-specific T cells late in infection when T-cell exhaustion has begun. Consistent with this is the finding that expression of programmed death-ligand 1 on APC isolated from LCMV-infected *fgl2*$^{+/+}$ *and fgl2*$^{-/-}$ mice at days 1 and 2 was not different (data not shown). This suggests that FGL2 could be involved in the contraction of cells rather than their expansion. Although naive T cells do not express FcγRIIB/RIII, virus-activated T cells have been shown to express FcγRIIB/RIII and hence the immunosuppressive effects of FGL2 on T cells in the setting of LCMV infection may be both direct and indirect.[23–25]

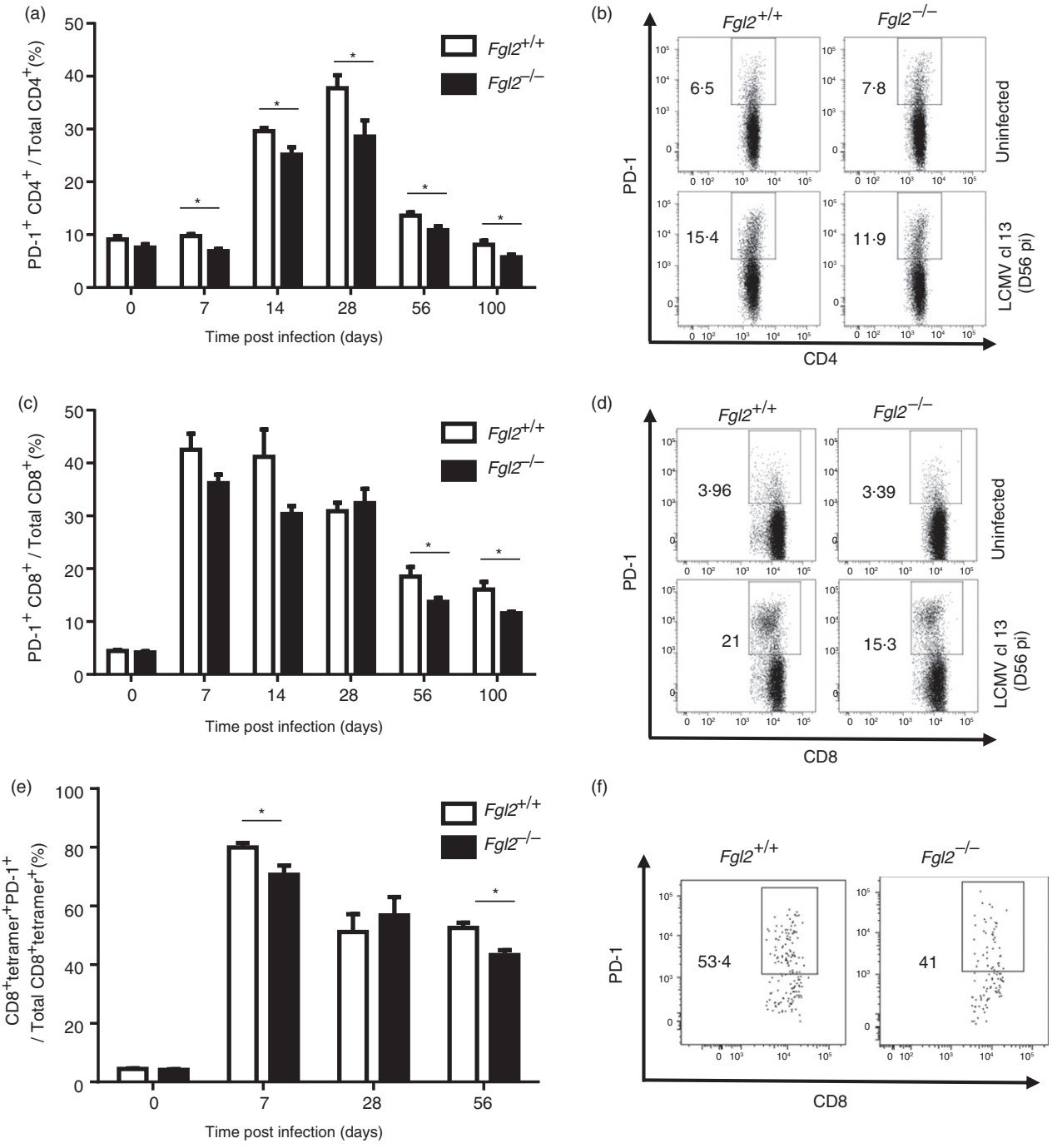

Figure 5. *Fgl2*$^{-/-}$ mice have reduced frequency (%) of programmed cell death protein 1 (PD-1) expressing CD4$^+$ and CD8$^+$ T cells following infection with lymphocytic choriomeningitis virus clone 13 (LCMV cl-13). *Fgl2*$^{+/+}$ and *fgl2*$^{-/-}$ mice were infected with 2×10^6 PFU of LCMV cl-13 and PD-1 expression on CD4$^+$ T cells (a, b) and on CD8$^+$ T cells (c, d) were determined by flow cytometry. Representative flow plots for CD4$^+$ (b) and CD8$^+$ cells (d) are shown. The frequency of CD3$^+$ CD8$^+$ Tet$_{GP33-41}$$^+$ T cells expressing PD-1 was determined by flow cytometry (e) and a representative flow plot is shown (f). Data are presented as the mean ± SEM from five mice per group and per time-point from two independent experiments *$P < 0{\cdot}05$.

In the present study, we examined the contribution of the FGL2-FcγRIIB/RIII pathway to the establishment of chronic infection caused by LCMV cl-13. Plasma levels of FGL2 were significantly increased early after LCMV cl-13 infection and remained elevated at all time-points p.i. in contrast to infection with LCMV WE, which causes only a short self-limiting acute infection where FGL2 was only elevated early post infection and to a lesser extent.[33] Although we have reported that Treg cells are a major source of FGL2, other cells including macrophages and

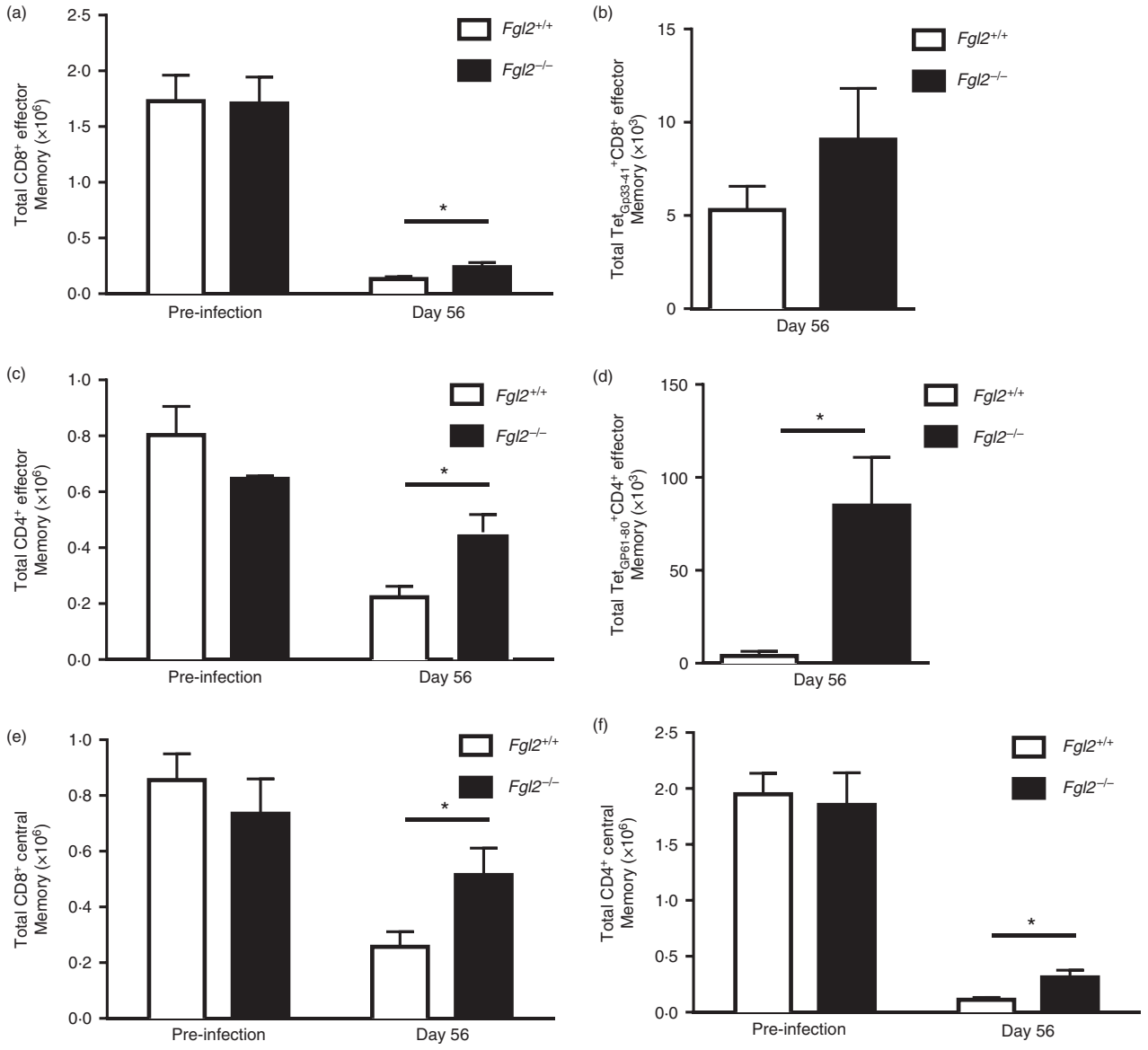

Figure 6. *Fgl2*$^{-/-}$ mice have increased central memory, effector memory after lymphocytic choriomeningitis virus clone 13 (LCMV cl-13) infection. Total CD8$^+$ (CD8$^+$ CD44^{high} CD62L^{low}) and CD4$^+$ (CD4$^+$ CD44^{high} CD62L^{low}) effector memory cells in the spleen in both *fgl2*$^{+/+}$ and *fgl2*$^{-/-}$ mice pre-infection and at day 56 post infection (p.i.) (a, c) were analysed. Virus-specific CD8$^+$ (CD8$^+$ Tet$_{Gp33\text{-}41}{}^+$ CD44^{high} CD62L^{low}) (b) and CD4$^+$ (CD4$^+$ Tet$_{Gp61\text{-}80}{}^+$ CD44^{high} CD62L^{low}) (d) effector memory cells were also determined at day 56 p.i. Total CD8$^+$ (CD8$^+$ CD44^{high} CD62L^{high}) and CD4$^+$ (CD4$^+$ CD44^{high} CD62L^{high}) central memory cells were determined from both *fgl2*$^{+/+}$ and *fgl2*$^{-/-}$ mice both pre-infection and at day 56 p.i. (e, f). Data are presented as the means ± SEM of five mice per group and time-point from three independent experiments *$P < 0{\cdot}05$.

CD8$^+$ T cells can produce FGL2. Hence at this time we cannot unequivocally state that increased FGL2 in the plasma is solely due to production by Treg.[22,51,52] We used mice that were genetically deficient in *fgl2* to study the effects of FGL2 on both the innate and adaptive antiviral immune response. Post LCMV cl-13 infection, *fgl2*$^{-/-}$ mice had increased numbers of macrophages and DC that expressed CD80, CD86 and MHC-II, markers of macrophage and DC activation in comparison with *fgl2*$^{+/+}$ mice. Early post LCMV infection at day 7, *fgl2*$^{+/+}$ generated a robust virus-specific T-cell response with enhanced numbers of CD3$^+$ CD8$^+$ Tet$_{GP33\text{-}41}{}^+$ T cells. However, by day 56, there was a significant contraction in both numbers of CD3$^+$ CD8$^+$ Tet$_{GP33\text{-}41}{}^+$ cells in *fgl2*$^{+/+}$ mice coupled with increased expression of PD-1 on both total and LCMV GP33-specific T cells, which was associated with reduced cellular and humoral antiviral activity and lower central and effector memory. In contrast, by day 56 p.i., *fgl2*$^{-/-}$ mice had increased frequencies of LCMV-specific CD3$^+$ CD8$^+$ Tet$_{GP33\text{-}41}{}^+$ T cells. CD8$^+$ and CD4$^+$

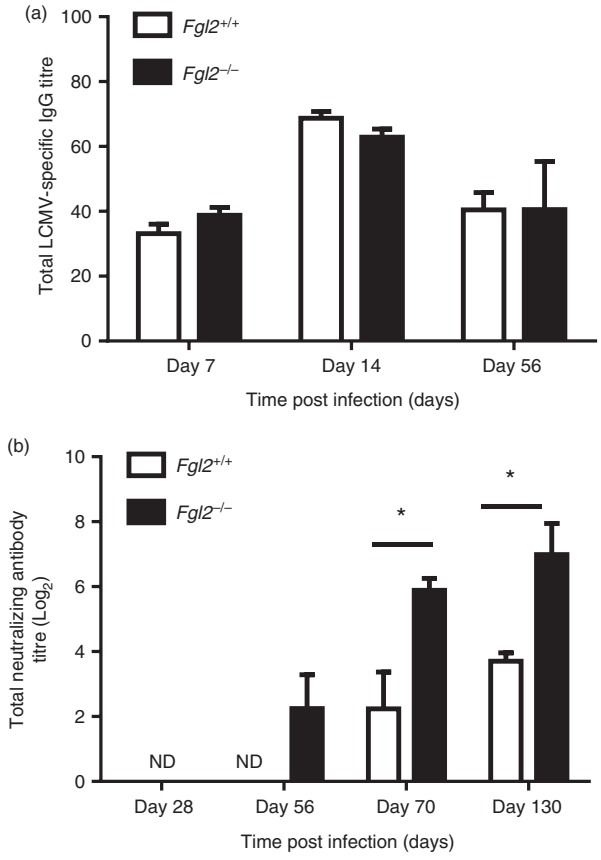

Figure 7. *Fgl2*$^{-/-}$ mice have enhanced production of neutralizing antibody after lymphocytic choriomeningitis virus clone 13 (LCMV cl-13) infection. Total LCMV-specific IgG was measured using an LCMV IgG specific ELISA (a). Data are presented as the mean absorbance at 450 nm × dilution of plasma ± SEM of five mice per group and per time-point from one independent experiment *$P < 0{\cdot}05$. (b) Total neutralizing antibody titres were measured in the plasma from LCMV-infected mice. The graph shows the dilution of plasma required for 50% plaque reduction of 200 PFU of LCMV cl-13 in a standard LCMV focus-forming assay. Data represent the $\log_2$ mean ± SEM of five mice per group and per time-point from one independent experiment *$P < 0{\cdot}05$.

T cells as well as LCMV-specific CD8$^+$ Tet$_{GP33\text{-}41}{}^+$ T cells from LCMV-infected *fgl2*$^{-/-}$ mice had reduced expression of PD-1, coincident with enhanced control of viral replication. This result is similar to what has been reported with disruption of interleukin-10.[15]

To firmly establish that binding of FGL2 to its receptor FcγRIIB/III accounted for changes in the innate and adaptive immune response to LCMV, mice chronically infected with LCMV were treated with antibody to FGL2 and FcγRIIB/III alone or in combination. Although treatment with either antibody alone partially restored virus-specific T-cell responses, these mice failed to clear LCMV. In contrast, treatment with combination of antibodies to both FGL2 and FcγRIIB/RIII led to restoration of CD4$^+$ and CD8$^+$ T-cell antiviral immunity and viral clearance. That antibody to FGL2 or FcγRIIB/RIII alone did not completely restore antiviral immunity and viral clearance may reflect that the dose and/or frequency of antibody administration might have been insufficient to fully neutralize FGL2. By increasing the dose and timing of administration, viral clearance may be possible, although this was not examined here. Alternatively, it has been reported that antibody administration in the setting of chronic viral infection is less effective, which was thought to be due to the generation of immune complexes.[53–56] The *fgl2*$^{-/-}$ mice generated high titred neutralizing antibody at days 70 and 130 p.i. and robust virus-specific central and effector T-cell and B-cell memory responses co-incident with viral clearance in the plasma, lung and liver by day 56. The changes in antibody concentration seen in this study may reflect differences in follicular T-cell helper function, which was not examined in this study. Treatment of chronically infected *fgl2*$^{+/+}$ mice with combination antibody to FGL2 and FcγRIIB/RIII resulted in similar results. Interestingly, virus could still be detected in the kidneys of *fgl2*$^{-/-}$ mice and *fgl2*$^{+/+}$ mice treated with anti-FGL2 and anti-FcγRIIB/RIII. The significance of this finding is not totally clear, although similar findings are seen in patients with chronic HCV infection who clear virus from the plasma. This finding may explain why transplantation of organs from virus-infected individuals who have cleared the virus from the plasma is known to be associated with a risk of virus transmission.[57] This is supportive of the concept that establishment of a sustained virological response in HCV infection leads to immunological control of infection but not total viral eradication.[58]

Wherry *et al.* have previously reported an increase in *fgl2* mRNA transcripts in effector and exhausted virus-specific T cells and expression of FcγRIIB on effector T cells.[24] In chronic infection, patients with chronic HBV and HCV infection have increased plasma levels of FGL2, as well as increased frequencies of Treg cells expressing FGL2.[50,59] Increased FGL2 during chronic infection could influence T-cell responsiveness to antigen directly by binding FcγRIIB on activated effector T cells and promoting T-cell exhaustion or indirectly by binding Fc receptors on APC, preventing DC maturation and antigen presentation. In a study by Starbeck-Miller *et al.*, expression of FcγRIIB following challenge with LCMV cl-13 was associated with reduced cytotoxicity and reduced secondary expansion of memory CD8$^+$ T cells.[23] It is known that FcγRIIB is an inhibitory receptor widely expressed on DC and B cells and signals through immunoreceptor tyrosine-based inhibition motif phosphorylation, which causes the recruitment of SHIP leading to reduction in activation of DC and apoptosis of B cells.[25] Additionally, FGL2 has been shown to augment immunosuppression by increasing expression levels of PD-1 and CD39,

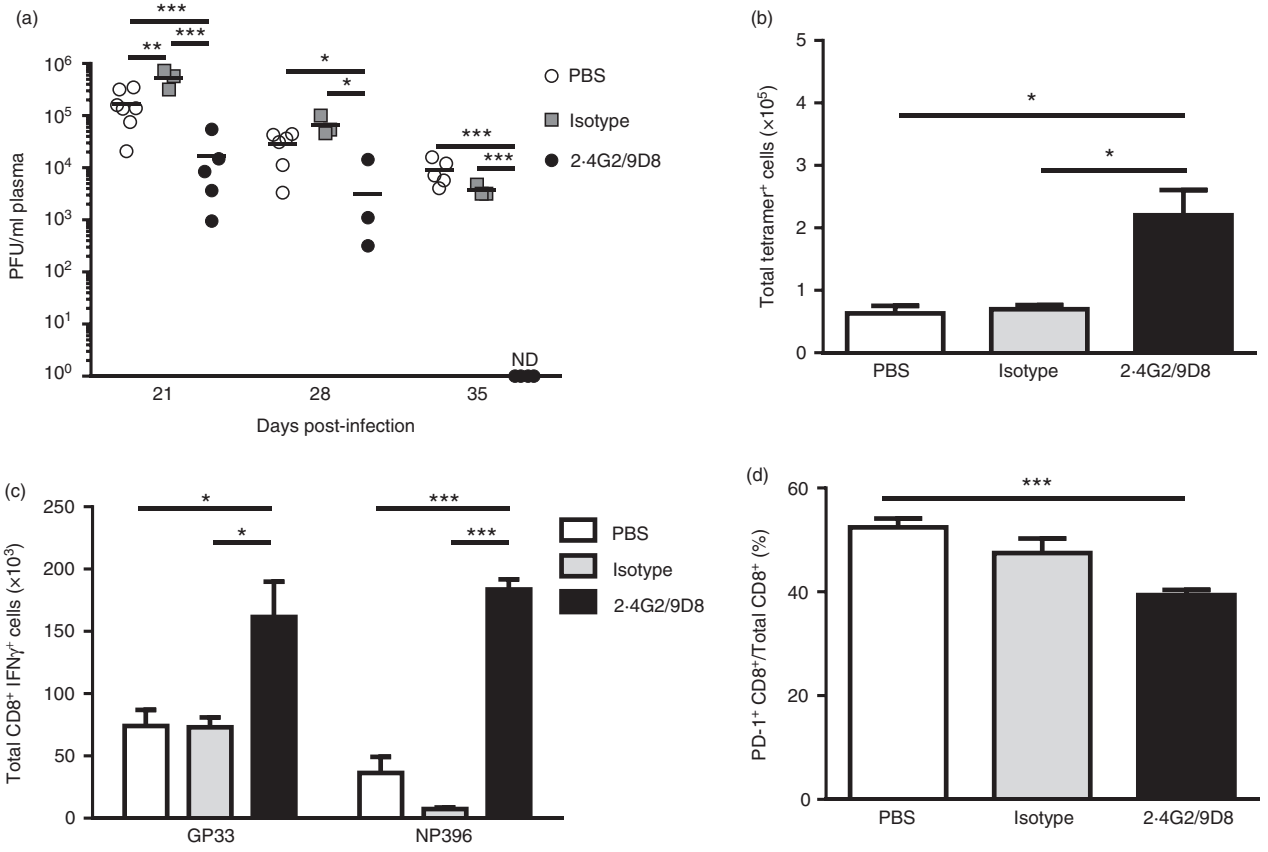

Figure 8. Pre-treatment with antibodies to fibrinogen-like protein 2 (FGL2) and FcγRIIB/RIII enhances $CD4^+$ and $CD8^+$ antiviral immunity with enhanced viral clearance. *Fgl2*$^{+/+}$ mice were pre-treated with 150 μg of neutralizing antibodies to FGL2 and 150 μg FcγRIIB/RIII (2.4G2/9D8), or 150 μg isotype control antibodies (150 μg of MOPC-21 and 150 μg 2A3), or 150 μl of PBS 2 days before infection. Mice were infected with 2×10^6 PFU of lymphocytic choriomeningitis virus clone 13 (LCMV cl-13) and subsequently treated with antibody or PBS every 2 days until day 20 p.i. Treatment with antibody or PBS was continued and given at days 23, 26, 32 and 45 p.i. Viral titres were determined in the plasma (a). The limit of detection of the LCMV focus-forming assay is denoted by the dashed line. Splenic mononuclear cells (SMNC) were isolated from 2.4G2/9D8, isotype control antibodies and PBS-treated mice at day 56 p.i. and stimulated with MHC-I restricted peptides and analysed by flow cytometry. Total numbers of $CD3^+$ $CD8^+$ $Tet_{GP33-41}{}^+$ T cells were determined (b). The total numbers of $CD3^+$ $CD8^+$ IFNγ^+ T cells responding to *ex vivo* peptide re-stimulation to GP_{33-41} or $NP_{396-404}$ was determined (c). The number of programmed cell death prtein 1 (PD-1) -expressing $CD3^+$ $CD8^+$ T cells was determined (d). Data are presented as the mean ± SEM of five mice per group from two independent experiments. $*P < 0{\cdot}05$ $***P < 0{\cdot}001$, $****P < 0{\cdot}0001$.

expanding the frequency of M2 macrophages through FcγRIIB, while increasing the number of myeloid-derived suppressor cells and Treg cells.[60]

In summary, the data presented here demonstrate an important role for FGL2 and FcγRIIB/RIII in the development of chronic LCMV cl-13 infection. Here, we show that targeted deletion of *fgl2* and treatment of *fgl2*$^{+/+}$ mice with neutralizing antibodies to FGL2 and FcγRIIB/RIII restores T-cell and B-cell antiviral immunity to LCMV cl-13, resulting in viral clearance. The studies support the concept that targeting the FGL2-FcγRIIB/RIII pathway might be useful to treat patients with chronic viral infections including HBV, HCV and HIV, which are known to induce expression of FGL2 and FcγRIIB/RIII.

Acknowledgements

We would like to thank Dr M. Oldstone for LCMV cl-13 and Dr P. Ohashi for the antibody to LCMV (VL4). Dr Nazia Selzner and Dr Gary Levy are recipients of grants from the Canadian Institute of Health Research (Grant 136781) and the Physician Services Incorporated (Grant 12-06).

Author contributions

OK, RK, DF, NY, KF, HS, JZ and OA performed the experiments. OK, RK, NS and GL were responsible for design of experiments, interpretation of data and writing the paper.

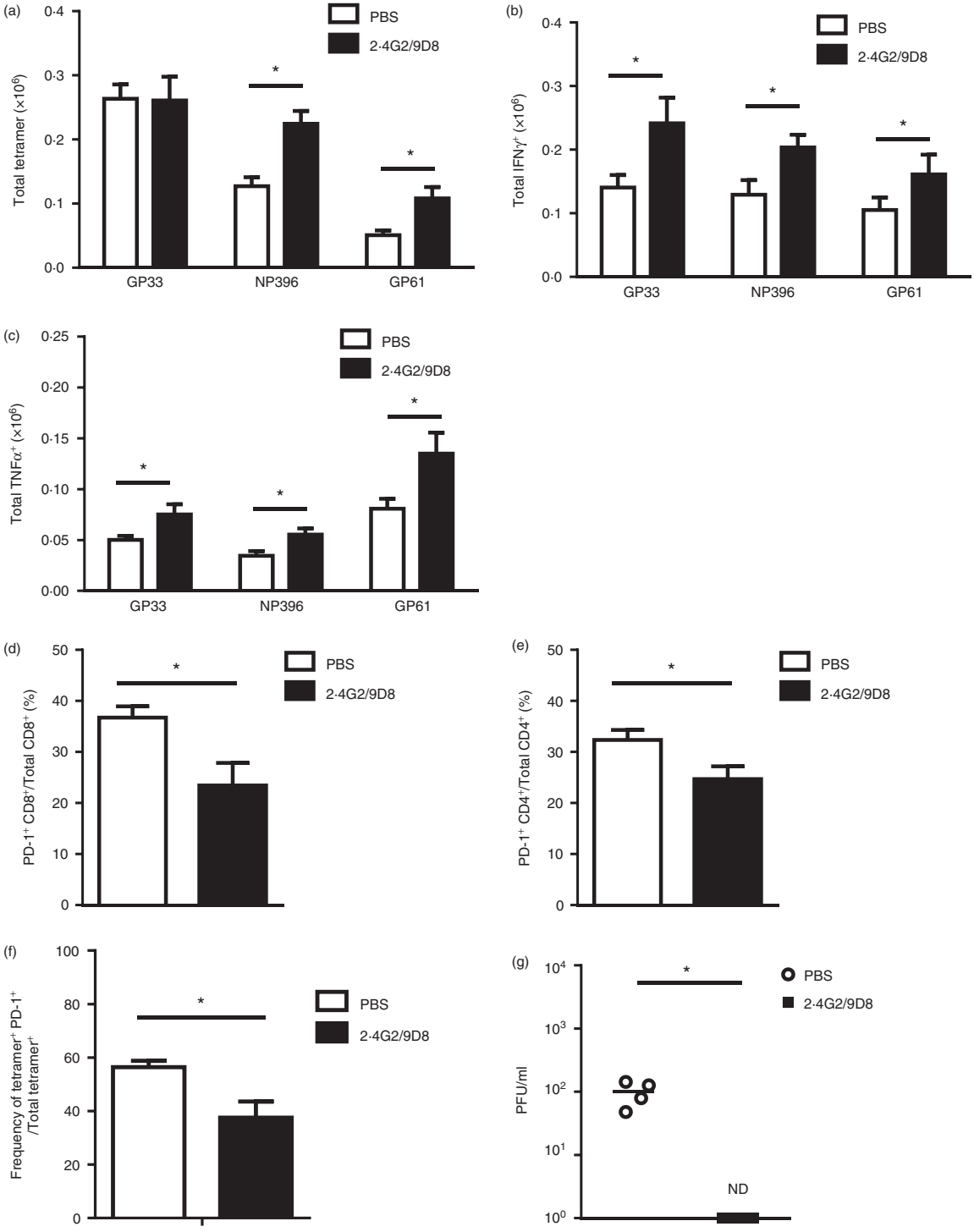

Figure 9. Treatment with antibody to fibrinogen-like protein 2 (FGL2) and FcγRIIB/RIII in mice chronically infected with lymphocytic choriomeningitis virus clone 13 (LCMV cl-13) enhances T-cell antiviral immunity and enhances viral clearance. *Fgl2*$^{+/+}$ mice were infected with 2×10^6 PFU of LCMV cl-13 and on day 25 post infection (p.i.) were treated with 150 μg of neutralizing antibody to FGL2 and 150 μg of neutralizing antibody to FcγRIIB/RIII (2.4G2/9D8) or 150 μl of PBS every 2 days until day 56 p.i. The total numbers of splenic $CD3^+$ $CD8^+$ $Tet_{Gp33\text{-}41}{}^+$, $CD3^+$ $CD8^+$ $Tet_{NP396\text{-}404}{}^+$ and $CD3^+$ $CD4^+$ $Tet_{GP61\text{-}80}{}^+$ were quantified by flow cytometry (a). Splenic mononuclear cells (SMNC) were isolated from antibody (2.4G2/9D8) and PBS-treated mice and were stimulated with MHC-I restricted peptides $GP_{33\text{-}41}$, $NP_{396\text{-}404}$ or the MHC-II restricted peptide $GP_{61\text{-}80}$ and production of intracellular $IFN\gamma^+$ (b) and TNF^+ (c) was measured. Frequencies of PD-1-expressing $CD3^+$ $CD8^+$ T cells (d),$CD3^+$ $CD4^+$ T cells (e) and $Tet_{GP33\text{-}41}{}^+$ $CD3^+$ $CD8^+$ T cells (f) were determined by flow cytometry. Plasma viral titres (g) were measured on day 56 p.i. The limit of detection of the LCMV focus-forming assay is denoted by the dashed line. Data are presented as the mean ± SEM of five mice per group from two independent experiments. $^*P < 0{\cdot}05$.

Conflicts of interest

The authors declare no conflicts of interest.

References

1 El-Serag HB. Epidemiology of viral hepatitis and hepatocellular carcinoma. *Gastroenterology* 2012; **142**:1264–73.e1.

2 Maartens G, Celum C, Lewin SR. HIV infection: epidemiology, pathogenesis, treatment, and prevention. *Lancet* 2014; **384**:258–71.

3 Barber DL, Wherry EJ, Masopust D, Zhu B, Allison JP, Sharpe AH *et al.* Restoring function in exhausted CD8 T cells during chronic viral infection. *Nature* 2006; **439**:682–7.

4 Chen JH, Perry CJ, Tsui YC, Staron MM, Parish IA, Dominguez CX *et al.* Prostaglandin E2 and programmed cell death 1 signaling coordinately impair CTL function and survival during chronic viral infection. *Nat Med* 2015; **21**:327–34.

5 Garidou L, Heydari S, Truong P, Brooks DG, McGavern DB. Therapeutic memory T cells require costimulation for effective clearance of a persistent viral infection. *J Virol* 2009; **83**:8905–15.

6 Jin HT, Anderson AC, Tan WG, West EE, Ha SJ, Araki K *et al.* Cooperation of Tim-3 and PD-1 in CD8 T-cell exhaustion during chronic viral infection. *Proc Natl Acad Sci U S A* 2010; **107**:14733–8.

7 Kasprowicz V, Schulze Zur Wiesch J, Kuntzen T, Nolan BE, Longworth S, Berical A *et al.* High level of PD-1 expression on hepatitis C virus (HCV)-specific $CD8^+$ and $CD4^+$ T cells during acute HCV infection, irrespective of clinical outcome. *J Virol* 2008; **82**:3154–60.

8 Blackburn SD, Shin H, Haining WN, Zou T, Workman CJ, Polley A *et al.* Coregulation of $CD8^+$ T cell exhaustion by multiple inhibitory receptors during chronic viral infection. *Nat Immunol* 2009; **10**:29–37.

9 Gallimore A, Glithero A, Godkin A, Tissot AC, Pluckthun A, Elliott T *et al.* Induction and exhaustion of lymphocytic choriomeningitis virus-specific cytotoxic T lymphocytes visualized using soluble tetrameric major histocompatibility complex class I-peptide complexes. *J Exp Med* 1998; **187**:1383–93.

10 Wherry EJ, Blattman JN, Murali-Krishna K, van der Most R, Ahmed R. Viral persistence alters CD8 T-cell immunodominance and tissue distribution and results in distinct stages of functional impairment. *J Virol* 2003; **77**:4911–27.

11 Bucks CM, Norton JA, Boesteanu AC, Mueller YM, Katsikis PD. Chronic antigen stimulation alone is sufficient to drive $CD8^+$ T cell exhaustion. *J Immunol* 2009; **182**:6697–708.

12 Welsh RM. Assessing CD8 T cell number and dysfunction in the presence of antigen. *J Exp Med* 2001; **193**:F19–22.

13 Ejrnaes M, Filippi CM, Martinic MM, Ling EM, Togher LM, Crotty S *et al.* Resolution of a chronic viral infection after interleukin-10 receptor blockade. *J Exp Med* 2006; **203**:2461–72.

14 Brown JA, Dorfman DM, Ma FR, Sullivan EL, Munoz O, Wood CR *et al.* Blockade of programmed death-1 ligands on dendritic cells enhances T cell activation and cytokine production. *J Immunol* 2003; **170**:1257–66.

15 Brooks DG, Trifilo MJ, Edelmann KH, Teyton L, McGavern DB, Oldstone MB. Interleukin-10 determines viral clearance or persistence *in vivo*. *Nat Med* 2006; **12**:1301–9.

16 Sakthivel P, Gereke M, Bruder D. Therapeutic intervention in cancer and chronic viral infections: antibody mediated manipulation of PD-1/PD-L1 interaction. *Rev Recent Clin Trials* 2012; **7**:10–23.

17 Cusick MF, Schiller JJ, Gill JC, Eckels DD. Hepatitis C virus induces regulatory T cells by naturally occurring viral variants to suppress T cell responses. *Clin Dev Immunol* 2011; **2011**:806061.

18 Peng G, Li S, Wu W, Sun Z, Chen Y, Chen Z. Circulating $CD4^+$ $CD25^+$ regulatory T cells correlate with chronic hepatitis B infection. *Immunology* 2008; **123**:57–65.

19 Punkosdy GA, Blain M, Glass DD, Lozano MM, O'Mara L, Dudley JP *et al.* Regulatory T-cell expansion during chronic viral infection is dependent on endogenous retroviral superantigens. *Proc Natl Acad Sci U S A* 2011; **108**:3677–82.

20 Stoop JN, van der Molen RG, Baan CC, van der Laan LJ, Kuipers EJ, Kusters JG *et al.* Regulatory T cells contribute to the impaired immune response in patients with chronic hepatitis B virus infection. *Hepatology* 2005; **41**:771–8.

21 Cabrera R, Tu Z, Xu Y, Firpi RJ, Rosen HR, Liu C *et al.* An immunomodulatory role for $CD4^+CD25^+$ regulatory T lymphocytes in hepatitis C virus infection. *Hepatology* 2004; **40**:1062–71.

22 Joller N, Lozano E, Burkett PR, Patel B, Xiao S, Zhu C *et al.* Treg cells expressing the coinhibitory molecule TIGIT selectively inhibit proinflammatory Th1 and Th17 cell responses. *Immunity* 2014; **40**:569–81.

23 Starbeck-Miller GR, Badovinac VP, Barber DL, Harty JT. Cutting edge: expression of FcγRIIB tempers memory CD8 T cell function in vivo. *J Immunol* 2014; **192**:35–9.

24 Wherry EJ, Ha SJ, Kaech SM, Haining WN, Sarkar S, Kalia V *et al.* Molecular signature of $CD8^+$ T cell exhaustion during chronic viral infection. *Immunity* 2007; **27**:670–84.

25 Huang ZY, Hunter S, Kim MK, Indik ZK, Schreiber AD. The effect of phosphatases SHP-1 and SHIP-1 on signaling by the ITIM- and ITAM-containing Fcgγ receptors FcγRIIB and FcγRIIA. *J Leukoc Biol* 2003; **73**:823–9.

26 Bolland S, Ravetch JV. Spontaneous autoimmune disease in FcγRIIB-deficient mice results from strain-specific epistasis. *Immunity* 2000; **13**:277–85.

27 Kyogoku C, Dijstelbloem HM, Tsuchiya N, Hatta Y, Kato H, Yamaguchi A *et al.* Fcγ receptor gene polymorphisms in Japanese patients with systemic lupus erythematosus: contribution of FCGR2B to genetic susceptibility. *Arthritis Rheum* 2002; **46**:1242–54.

28 Iruretagoyena MI, Riedel CA, Leiva ED, Gutierrez MA, Jacobelli SH, Kalergis AM. Activating and inhibitory Fcγ receptors can differentially modulate T cell-mediated autoimmunity. *Eur J Immunol* 2008; **38**:2241–50.

29 Araujo-Jorge T, Rivera MT, el Bouhdidi A, Daeron M, Carlier Y. An FcγRII-, FcγRIII-specific monoclonal antibody (2.4G2) decreases acute *Trypanosoma cruzi* infection in mice. *Infect Immun* 1993; **61**:4925–8.

30 Gjertsson I, Kleinau S, Tarkowski A. The impact of Fcγ receptors on *Staphylococcus aureus* infection. *Microb Pathog* 2002; **33**:145–52.

31 Clatworthy MR, Smith KG. FcγRIIb balances efficient pathogen clearance and the cytokine-mediated consequences of sepsis. *J Exp Med* 2004; **199**:717–23.

32 Shalev I, Wong KM, Foerster K, Zhu Y, Chan C, Maknojia A *et al.* The novel $CD4^+CD25^+$ regulatory T cell effector molecule fibrinogen-like protein 2 contributes to the outcome of murine fulminant viral hepatitis. *Hepatology* 2009; **49**:387–97.

33 Khattar R, Luft O, Yavorska N, Shalev I, Phillips MJ, Adeyi O *et al.* Targeted deletion of FGL2 leads to increased early viral replication and enhanced adaptive immunity in a murine model of acute viral hepatitis caused by LCMV WE. *PLoS ONE* 2013; **8**:e72309.

34 Shalev I, Liu H, Koscik C, Bartczak A, Javadi M, Wong KM *et al.* Targeted deletion of fgl2 leads to impaired regulatory T cell activity and development of autoimmune glomerulonephritis. *J Immunol* 2008; **180**:249–60.

35 Battegay M, Cooper S, Althage A, Banziger J, Hengartner H, Zinkernagel RM. Quantification of lymphocytic choriomeningitis virus with an immunological focus assay in 24- or 96-well plates. *J Virol Methods* 1991; **33**:191–8.

36 Takimoto K, Taharaguchi M, Morikawa S, Ike F, Yamada YK. Detection of the antibody to lymphocytic choriomeningitis virus in sera of laboratory rodents infected with viruses of laboratory and newly isolated strains by ELISA using purified recombinant nucleoprotein. *Exp Anim* 2008; **57**:357–65.

37 Battegay M, Moskophidis D, Waldner H, Brundler MA, Fung-Leung WP, Mak TW *et al.* Impairment and delay of neutralizing antiviral antibody responses by virus-specific cytotoxic T cells. *J Immunol* 1993; **151**:5408–15.

38 Coligan JE, Kruisbeek AM, Margulies DH, Shevach EM, Strober W (eds) Current Protocols in Immunology. New York: John Wiles & Sons, Inc., 1998.

39 Jackson HM, Dimopoulos N, Chen Q, Luke T, Yee Tai T, Maraskovsky E, *et al.* A robust human T-cell culture method suitable for monitoring $CD8^+$ and $CD4^+$ T-cell responses from cancer clinical trial samples. *J Immunol Methods* 2004; **291**:51–62.

40 Rydyznski C, Daniels KA, Karmele EP, Brooks TR, Mahl SE, Moran MT, *et al.* Generation of cellular immune memory and B-cell immunity is impaired by natural killer cells. *Nat Commun* 2015; **6**:6375.

41 Dimopoulos N, Jackson HM, Ebert L, Guillaume P, Luescher IF, Ritter G, *et al.* Combining MHC tetramer and intracellular cytokine staining for $CD8^+$ T cells to reveal antigenic epitopes naturally presented on tumor cells. *J Immunol Methods* 2009; **340**:90–4.

42 Rose S, Misharin A, Perlman H. A novel Ly6C/Ly6G-based strategy to analyze the mouse splenic myeloid compartment. *Cytometry A* 2012; **81**:343–50.

43 Chan CW, Kay LS, Khadaroo RG, Chan MW, Lakatoo S, Young KJ, *et al.* Soluble fibrinogen-like protein 2/fibroleukin exhibits immunosuppressive properties: suppressing T cell proliferation and inhibiting maturation of bone marrow-derived dendritic cells. *J Immunol* 2003; **170**:4036–44.

44 Brooks DG, Ha SJ, Elsaesser H, Sharpe AH, Freeman GJ, Oldstone MB. IL-10 and PD-L1 operate through distinct pathways to suppress T-cell activity during persistent viral infection. *Proc Natl Acad Sci U S A* 2008; **105**:20428–33.

45 Penaloza-MacMaster P, Kamphorst AO, Wieland A, Araki K, Iyer SS, West EE, *et al.* Interplay between regulatory T cells and PD-1 in modulating T cell exhaustion and viral control during chronic LCMV infection. *J Exp Med* 2014; **211**:1905.

46 West EE, Jin H-T, Rasheed A-U, Penaloza-MacMaster P, Ha S-J, Tan WG, *et al.* PD-L1 blockade synergizes with IL-2 therapy in reinvigorating exhausted T cells. *J Clin Invest* 2013; **123**:2604–15.

47 Starbeck-Miller GR, Xue H-H, Harty JT. IL-12 and type I interferon prolong the division of activated CD8 T cells by maintaining high-affinity IL-2 signaling *in vivo*. *J Exp Med* 2014; **211**:105–20.

48 Oldstone MB. Anatomy of viral persistence. *PLoS Pathog* 2009; **5**:e1000523.

49 Liu H, Shalev I, Manuel J, He W, Leung E, Crookshank J, *et al.* The FGL2-FcγRIIB pathway: a novel mechanism leading to immunosuppression. *Eur J Immunol* 2008; **38**:3114–26.

50 Foerster K, Helmy A, Zhu Y, Khattar R, Adeyi OA, Wong KM, *et al.* The novel immunoregulatory molecule FGL2: a potential biomarker for severity of chronic hepatitis C virus infection. *J Hepatol* 2010; **53**:608–15.
51 Urbanellis P, Shyu W, Khattar R, Wang J, Zakharova A, He W, *et al.* The regulatory T cell effector molecule fibrinogen-like protein 2 is necessary for the development of rapamycin-induced tolerance to fully MHC-mismatched murine cardiac allografts. *Immunology* 2015; **144**:91–106.
52 Bartczak A, Zhang J, Adeyi O, Amir A, Grant D, Gorczynski R, *et al.* Overexpression of fibrinogen-like protein 2 protects against T cell-induced colitis. *World J Gastroenterol* 2017; **23**:2673–84.
53 Yamada DH, Elsaesser H, Lux A, Timmerman JM, Morrison SL, de la Torre JC, *et al.* Suppression of Fcγ-receptor-mediated antibody effector function during persistent viral infection. *Immunity* 2015; **42**:379–90.
54 Wieland A, Shashidharamurthy R, Kamphorst AO, Han JH, Aubert RD, Choudhury BP, *et al.* Antibody effector functions mediated by Fcγ-receptors are compromised during persistent viral infection. *Immunity* 2015; **42**:367–78.
55 Trépanier P, Chabot D, Bazin R. Intravenous immunoglobulin modulates the expansion and cytotoxicity of $CD8^+$ T cells. *Immunology* 2014; **141**:233–41.
56 Aubin E, Lemieux R, Bazin R. Indirect inhibition of *in vivo* and *in vitro* T-cell responses by intravenous immunoglobulins due to impaired antigen presentation. *Blood* 2010; **115**:1727–34.
57 Levitsky J, Doucette K. Viral hepatitis in solid organ transplantation. *Am J Transplant* 2013; **4**:147–68.
58 Recher M, Lang KS, Navarini A, Hunziker L, Lang PA, Fink K, *et al.* Extralymphatic virus sanctuaries as a consequence of potent T-cell activation. *Nat Med* 2007; **13**:1316–23.
59 Shalev I, Selzner N, Helmy A, Foerster K, Adeyi OA, Grant DR, *et al.* The role of FGL2 in the pathogenesis and treatment of hepatitis C virus infection. *Rambam Maimonides Med J* 2010; **1**:e0004.
60 Yan J, Kong LY, Hu J, Gabrusiewicz K, Dibra D, Xia X, *et al.* FGL2 as a multimodality regulator of tumor-mediated immune suppression and therapeutic target in gliomas. *J Natl Cancer Inst* 2015; **107**:djv137.

Supporting Information

Additional Supporting Information may be found in the online version of this article:

Fig. S1. Gating strategy for macrophage and dendritic cells.

Fig. S2. Characterization of the anti-fibrinogen-like protein 2 antibody 9D8.

Fig. S3. Gating strategy for $CD8^+$ lymphocytic choriomeningitis virus-specific memory cells.